

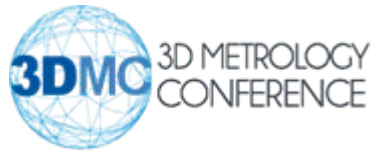


Two Uncertainty Models for Spherical Instrument Measurements

John Dorsey-Palmateer

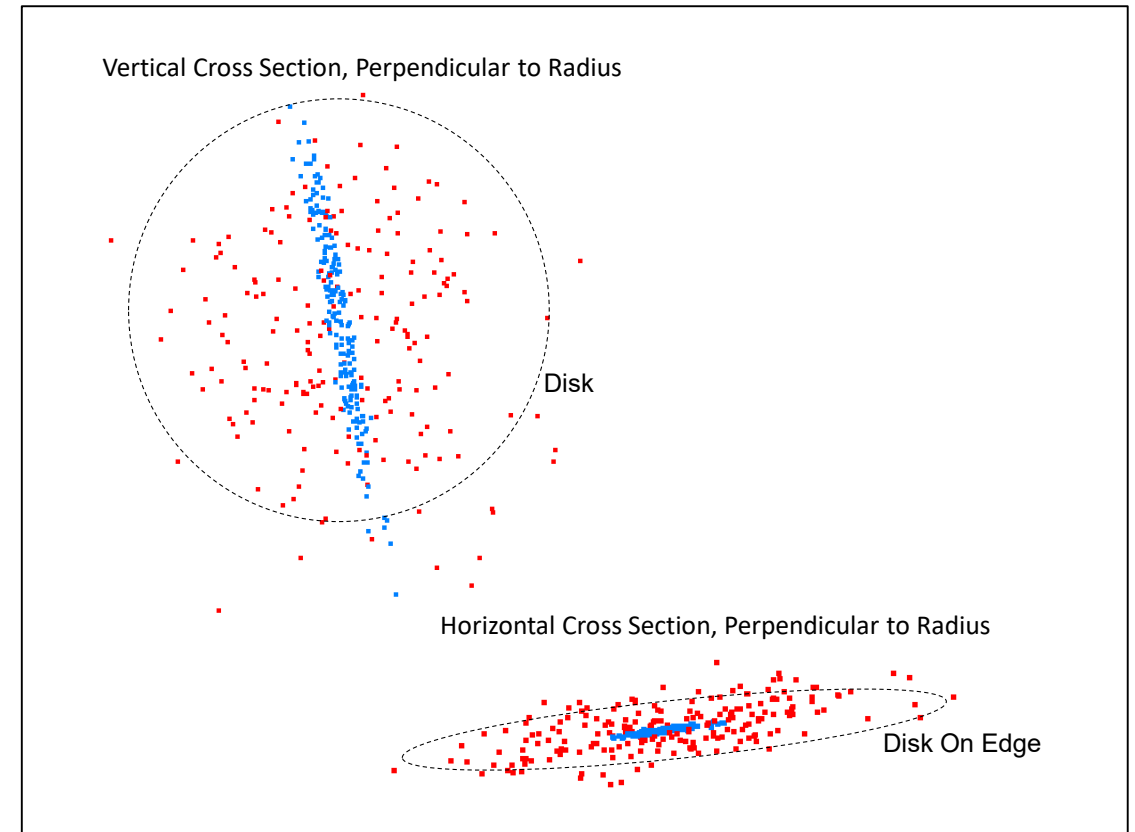
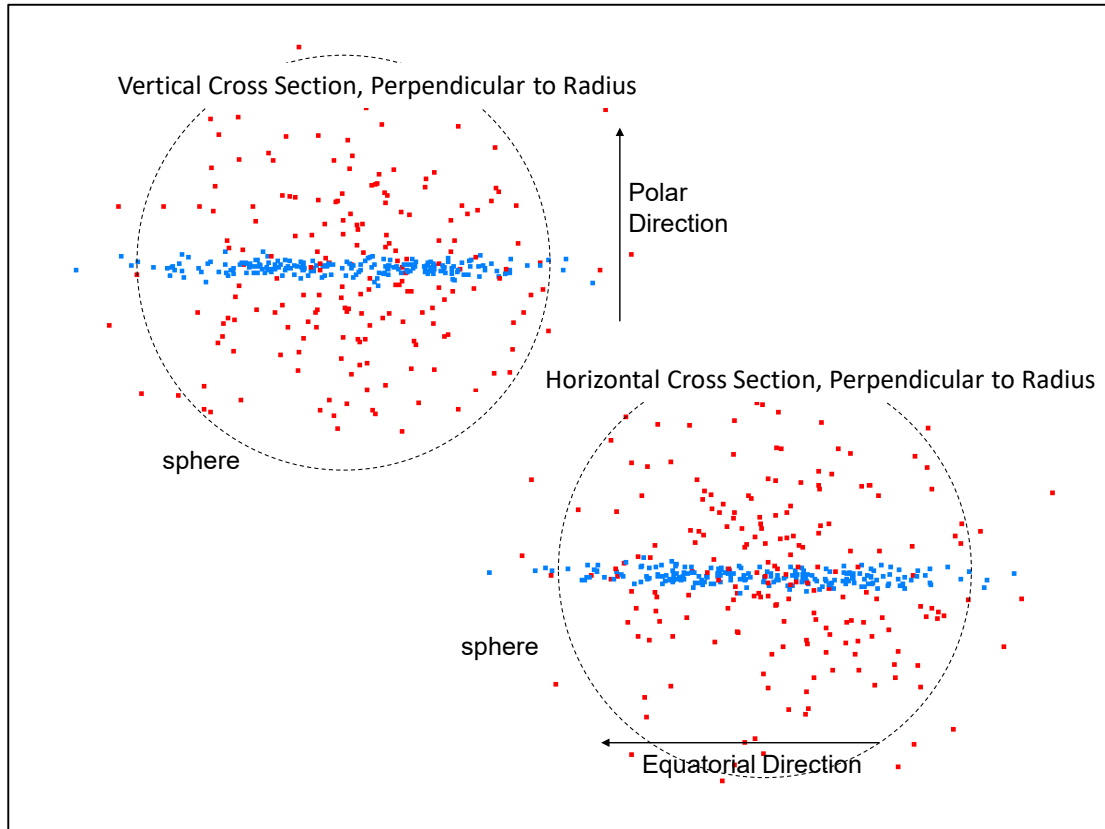
JDP Metrology Consulting, LLC

3D Metrology Conference – 3DMC



2018 Hamburg GERMANY

Background





Today

Cerro Pachón, Chile 2647 m (8684 ft)

LSST Project/NSF/AURA



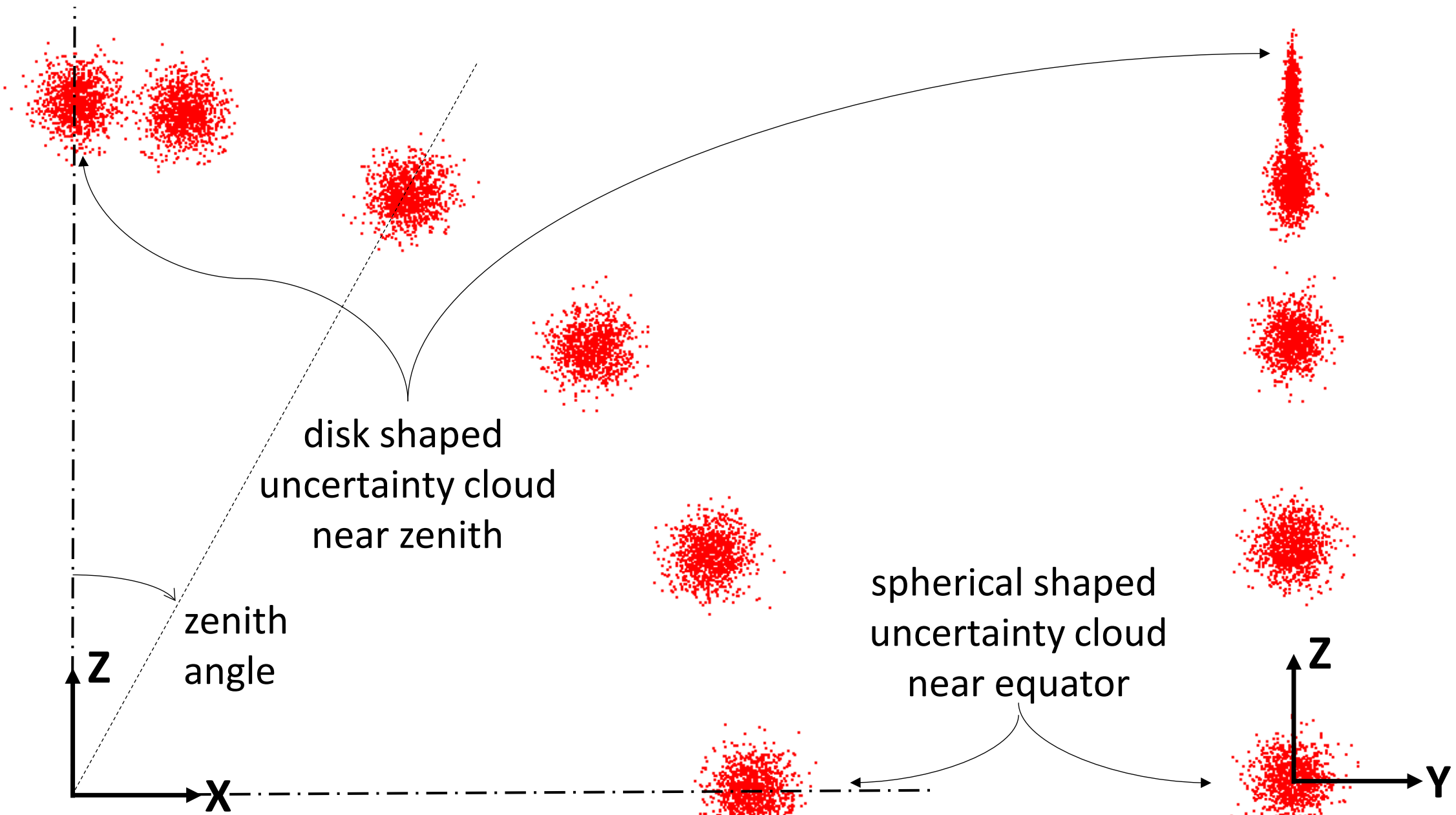
LSST Project/NSF/AURA





Monte Carlo Uncertainty

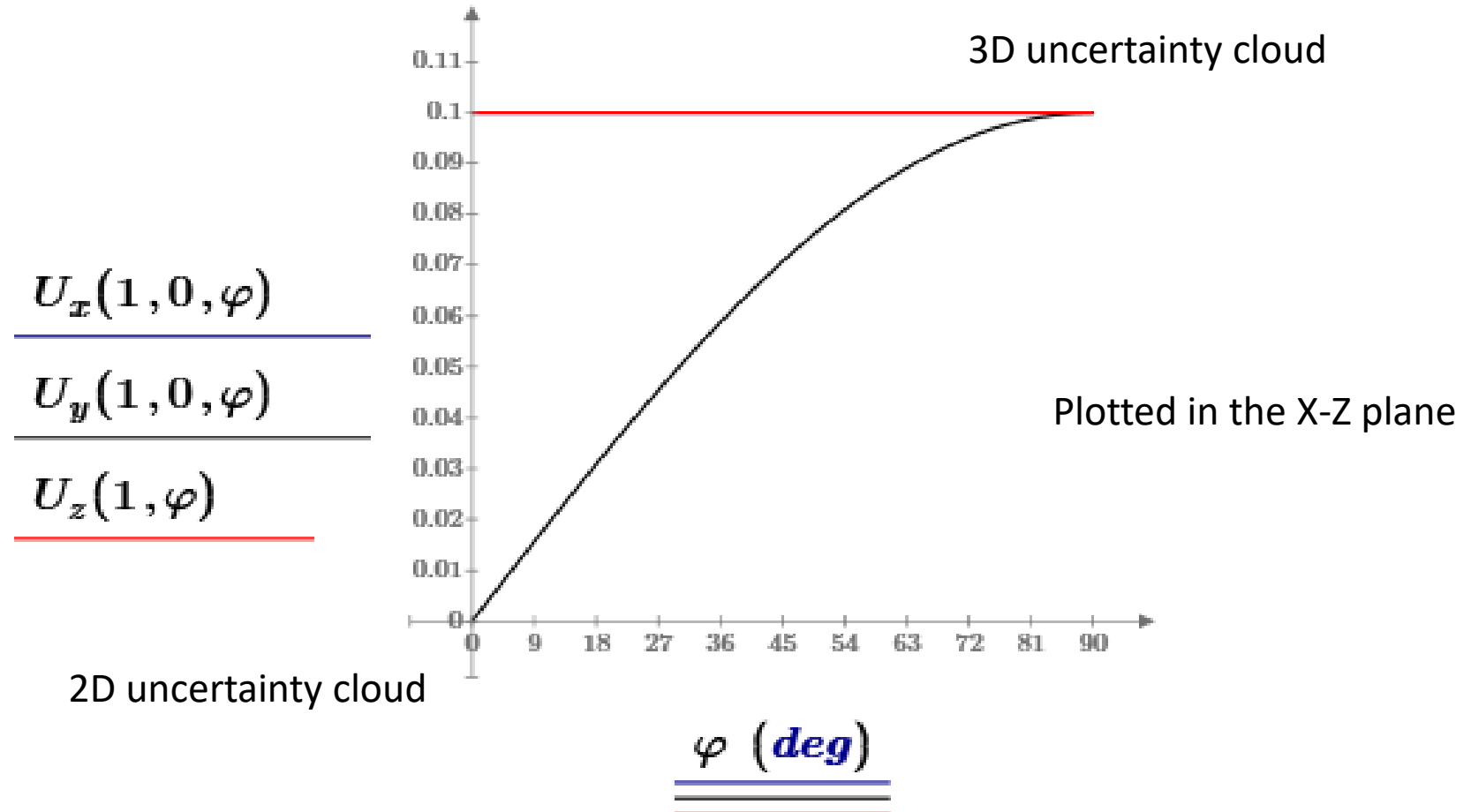
- Starting with the Spherical to Cartesian transformation, iteratively add errors Δr , $\Delta \theta$ and $\Delta \varphi$ to the range and angles
 - $\Delta x(r, \theta, \varphi) = (r + \Delta r) \cos(\theta + \Delta \theta) \sin(\varphi + \Delta \varphi)$
 - $\Delta y(r, \theta, \varphi) = (r + \Delta r) \sin(\theta + \Delta \theta) \sin(\varphi + \Delta \varphi)$
 - $\Delta z(r, \varphi) = (r + \Delta r) \cos(\varphi + \Delta \varphi)$



Linear Propagation of Errors

- $U_x(r, \theta, \varphi) = \sqrt{D_{\Delta r}x(r, \theta, \varphi)^2 \cdot \Delta r^2 + D_{\Delta \theta}x(r, \theta, \varphi)^2 \cdot \Delta \theta^2 + D_{\Delta \varphi}x(r, \theta, \varphi)^2 \cdot \Delta \varphi^2}$
- $U_y(r, \theta, \varphi) = \sqrt{D_{\Delta r}y(r, \theta, \varphi)^2 \cdot \Delta r^2 + D_{\Delta \theta}y(r, \theta, \varphi)^2 \cdot \Delta \theta^2 + D_{\Delta \varphi}y(r, \theta, \varphi)^2 \cdot \Delta \varphi^2}$
- $U_z(r, \varphi) = \sqrt{D_{\Delta r}z(r, \varphi)^2 \cdot \Delta r^2 + D_{\Delta \varphi}z(r, \varphi)^2 \cdot \Delta \varphi^2}$

Linear Propagation of Errors





Discussion

- Intuitively, the flattening at the poles made no sense
- Sighting through a theodolite telescope, visually there is lateral variation of the same order at all vertical angles: the field-of-view (FOV) does not squeeze into a plane
- The same is true for spherical instrument such as a tracking interferometer: both the receiver optics and quadrant detector in the tracker feedback loop have lateral variation at all angles.
- Something is amiss with the spherical to cartesian model

Instrument Convolution

- $m(t) = x(t) * \delta(t) = \int_{-\infty}^{\infty} x(\lambda) \cdot \delta(t - \lambda) d\lambda = x(t)$

- Tape Deck example

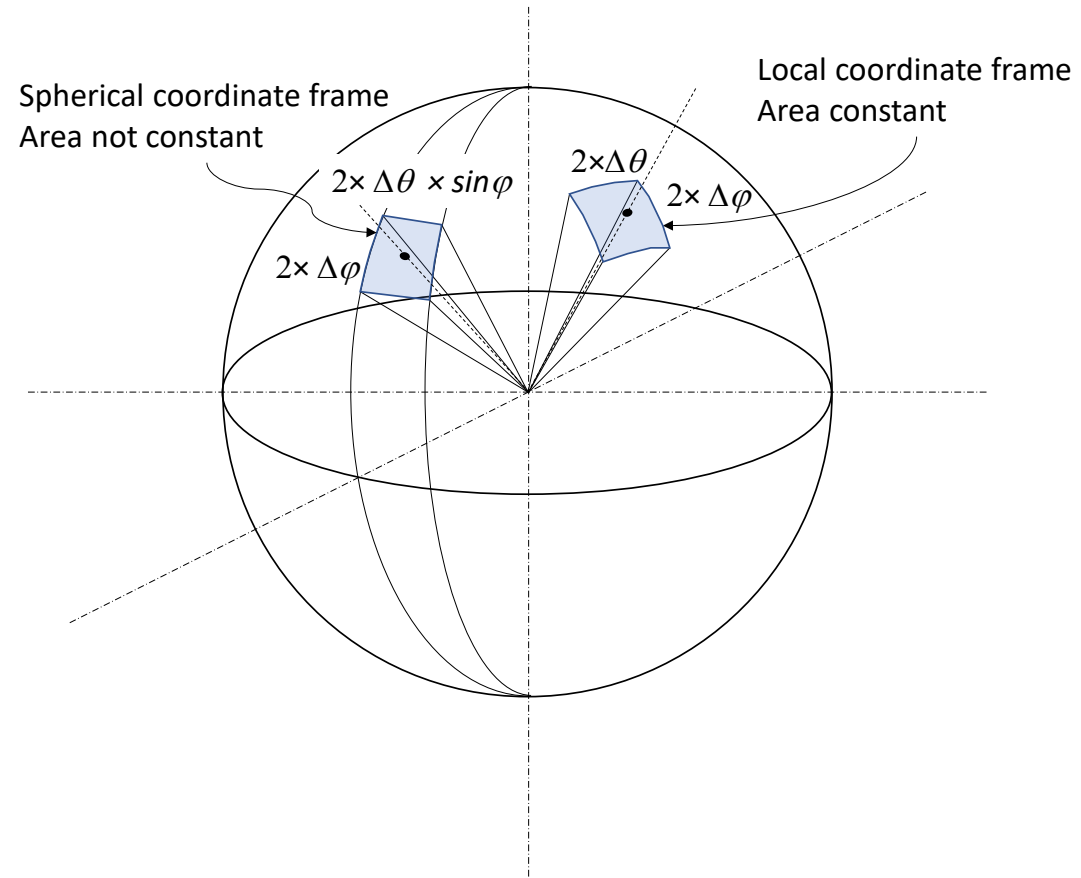
- $m(t) = \int_{t-\frac{T}{2}}^{t+\frac{T}{2}} x(\lambda) d\lambda = \int_{-\infty}^{t+\frac{T}{2}} x(\lambda) d\lambda - \int_{-\infty}^{t-\frac{T}{2}} x(\lambda) d\lambda$

- $m(t) = x(t) * \left(u\left(t + \frac{T}{2}\right) - u\left(t - \frac{T}{2}\right) \right)$

- Spherical Instrument (e.g. Telescope & Tracker) example

- $m(\theta, \varphi) = \int_{\theta-\Delta\theta}^{\theta+\Delta\theta} \int_{\varphi-\Delta\varphi}^{\varphi+\Delta\varphi} F(1, \lambda, \eta) d\eta d\lambda$

Uncertainty Regions with Constant Area

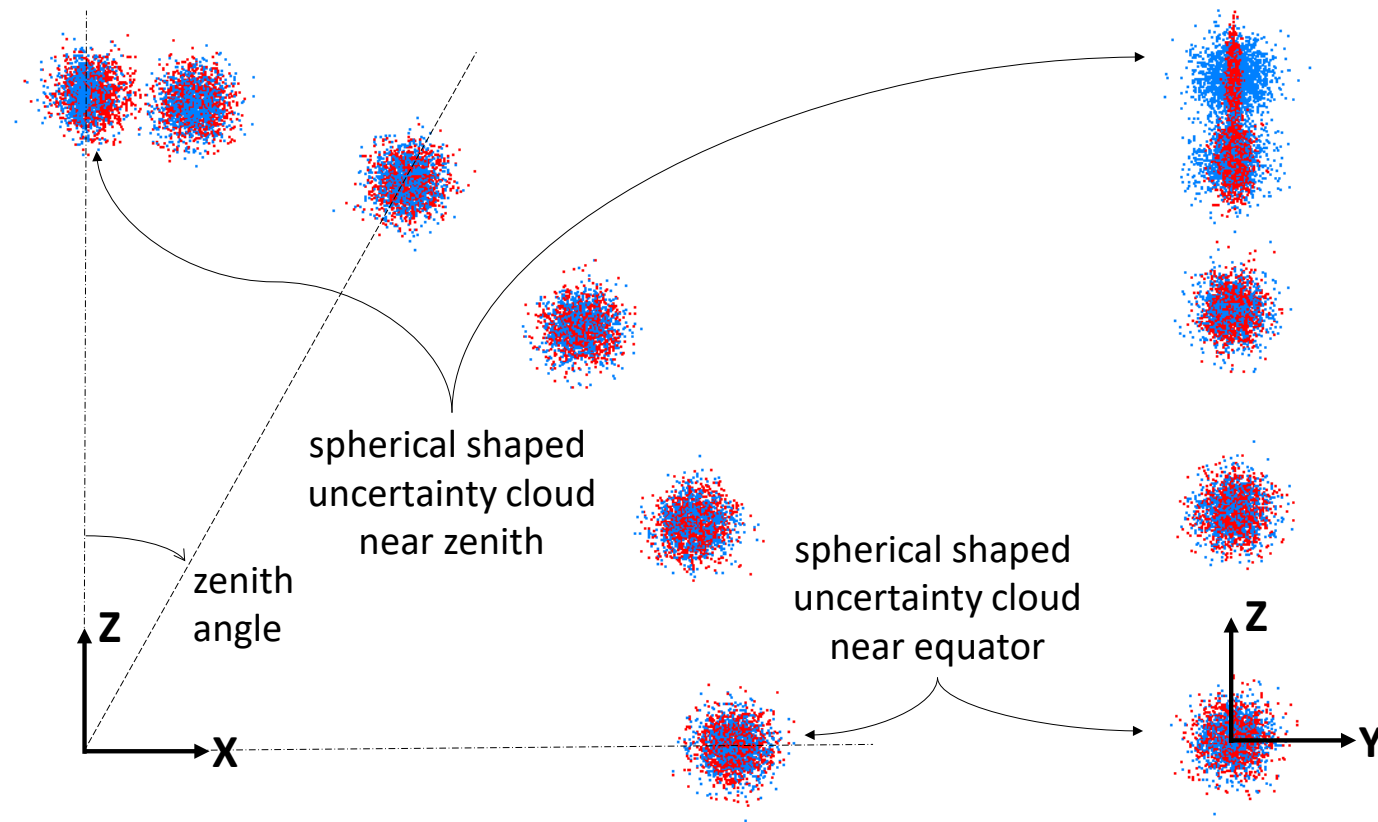




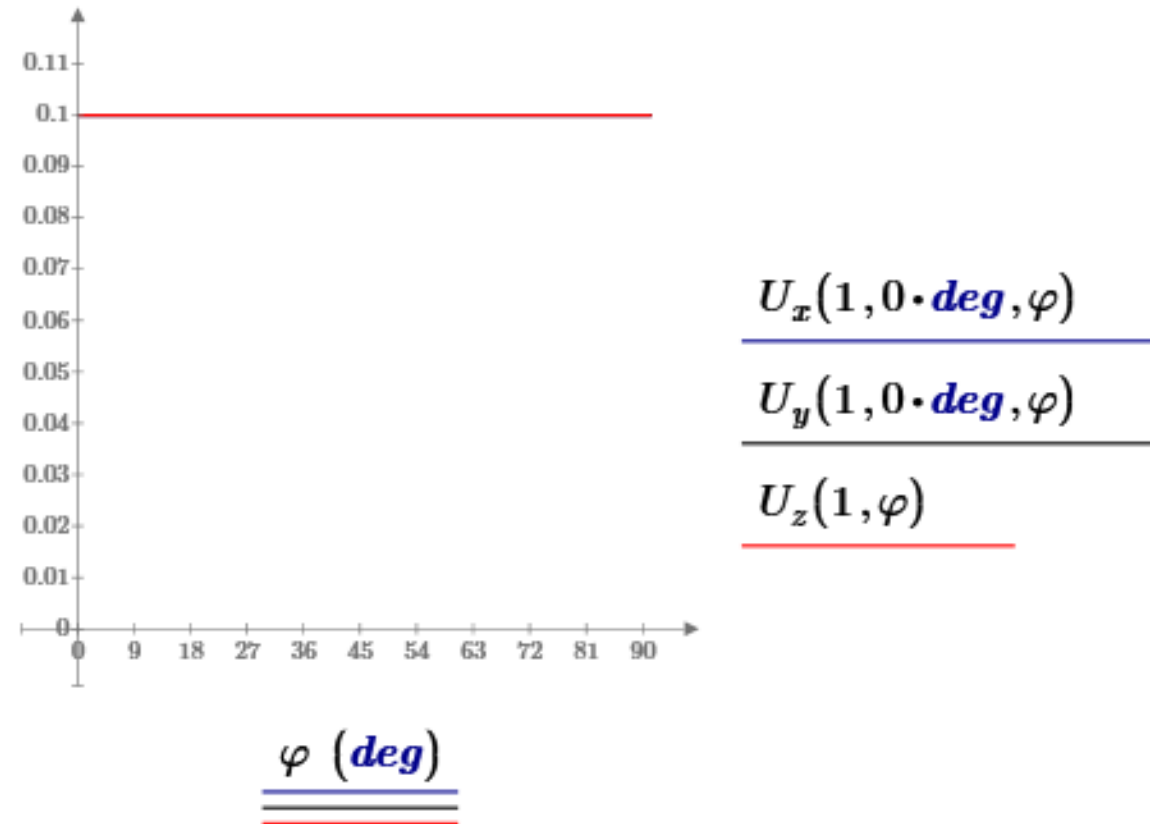
Vector Field Solution

- Measurement Vector (on-LOS) + Uncertainty Field (off-LOS)
- $$\Delta x(r, \theta, \varphi, \Delta r, \Delta \theta, \Delta \varphi) := r \cdot \sin(\varphi) \cdot \cos(\theta) \downarrow$$
$$+ \Delta r \cdot \sin(\varphi) \cdot \cos(\theta) - r \cdot \Delta \varphi \cdot \cos(\varphi) \cdot \cos(\theta) - r \cdot \Delta \theta \cdot \sin(\theta)$$
- $$\Delta y(r, \theta, \varphi, \Delta r, \Delta \theta, \Delta \varphi) := r \cdot \sin(\varphi) \cdot \sin(\theta) \downarrow$$
$$+ \Delta r \cdot \sin(\varphi) \cdot \sin(\theta) - r \cdot \Delta \varphi \cdot \cos(\varphi) \cdot \sin(\theta) + r \cdot \Delta \theta \cdot \cos(\theta)$$
- $$\Delta z(r, \varphi, \Delta r, \Delta \varphi) := r \cdot \cos(\varphi) \downarrow$$
$$+ \Delta r \cdot \cos(\varphi) + r \cdot \Delta \varphi \cdot \sin(\varphi)$$

Monte Carlo Uncertainty (compared)

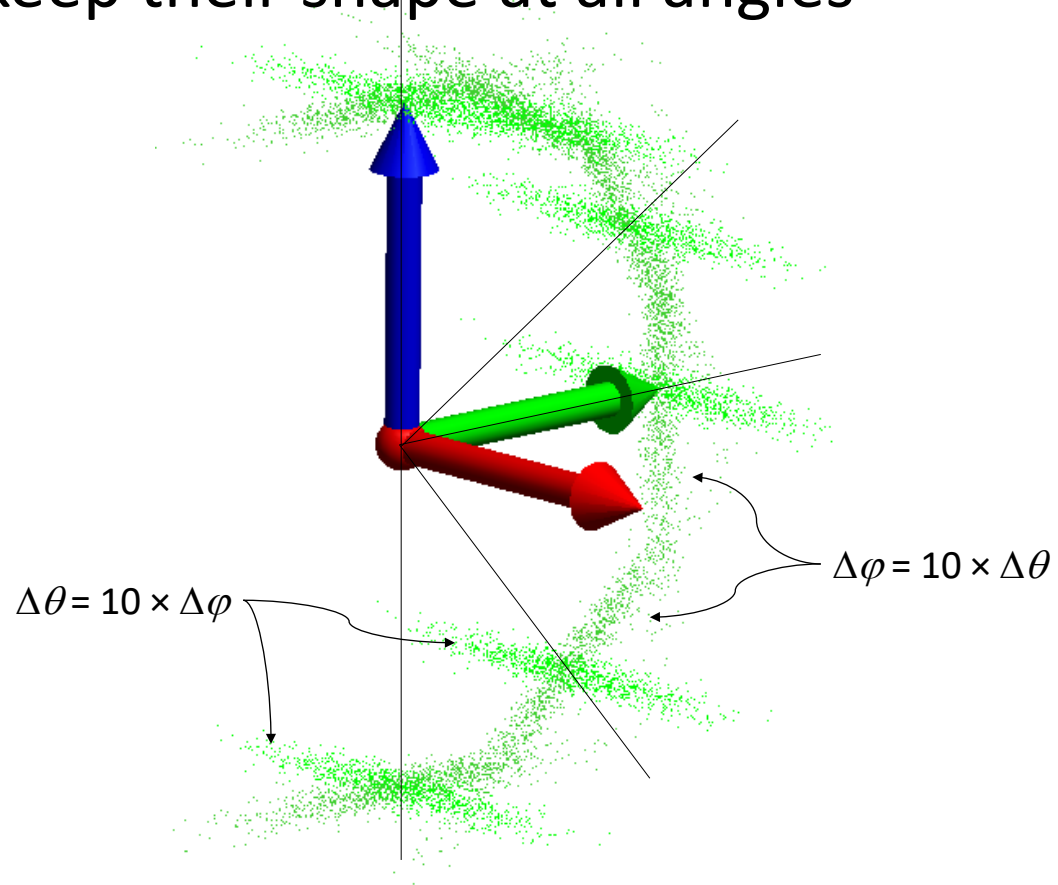


Linear Propagation of Errors



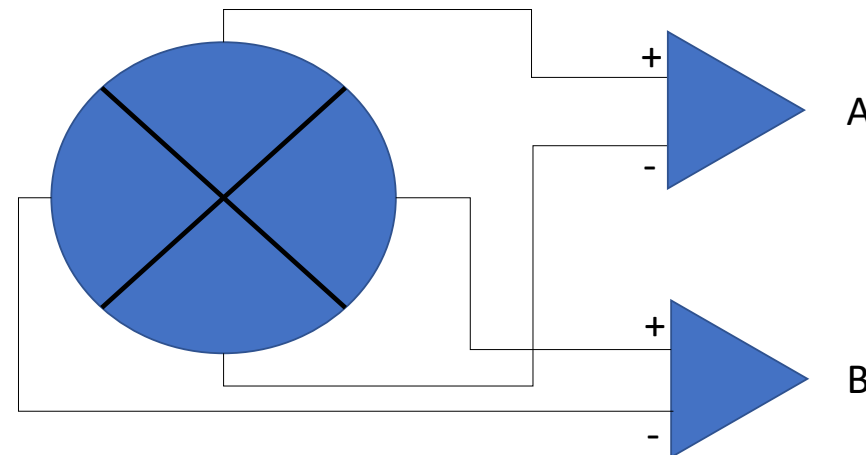
Robustness

- The point clouds keep their shape at all angles



Solution with Simple Kinematic Tracker Model using PSD Uncertainty

- Trackers PSD detects lateral error from the retro-reflector and drives servo motors, keeping the laser pointed at the retro-reflector
- The tracker PSD is the “aperture”
 - it senses the laser return
 - initiates control signals.

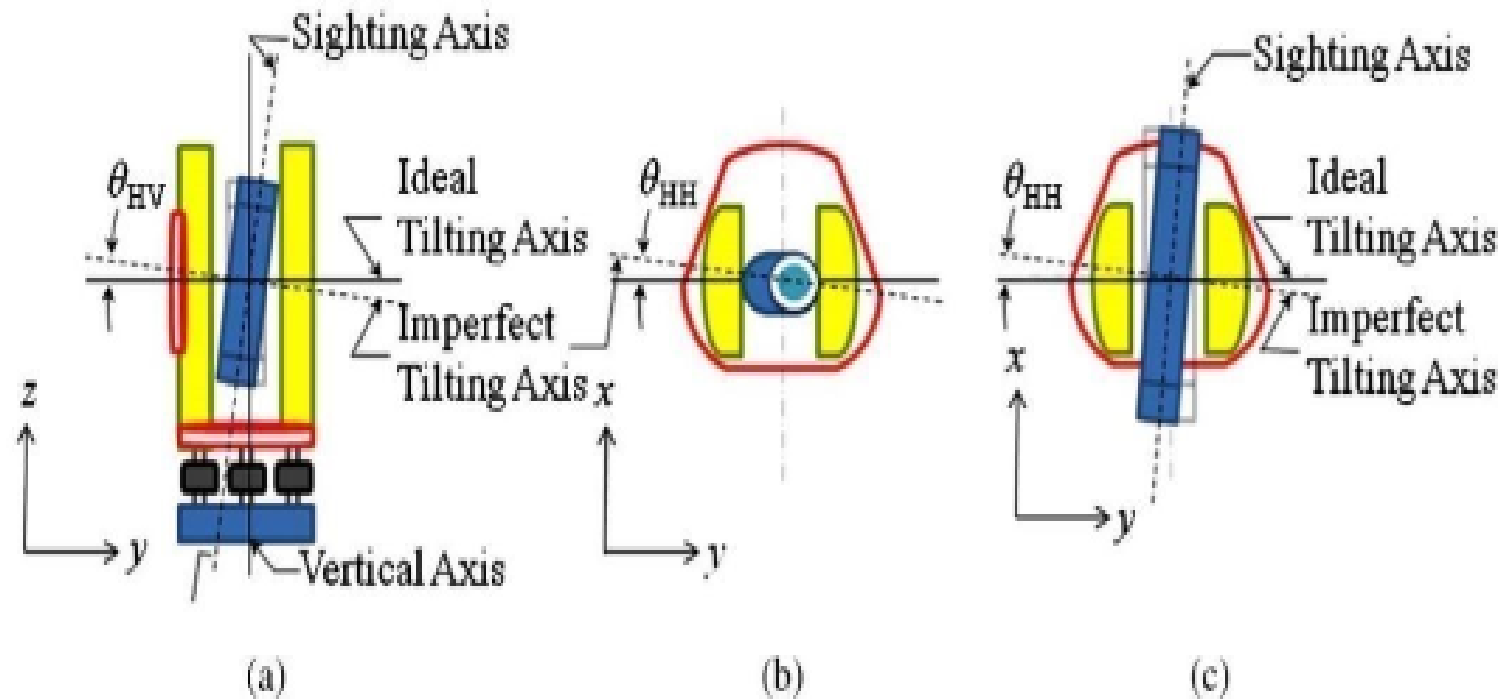


PSD and the Tracker

- The PSD does not rotate, so the azimuth angle, θ , keeps the A and B signals aligned with the alidade
 - $\begin{vmatrix} \Delta u \\ \Delta v \end{vmatrix} \approx \begin{vmatrix} \cos \theta & \sin \theta \\ -\sin \theta & \cos \theta \end{vmatrix} \times \begin{vmatrix} A \\ B \end{vmatrix}$
- Examining the values Δu and Δv with the tracker is pointing at the equator shows:
 - errors in the horizontal angle are proportional to Δu
 - errors in the zenith angle are proportional to Δv
- However, at zenith:
 - errors in the horizontal angle are not proportional to Δu
 - errors in the zenith angle remain proportional to Δv

Standing Axis Errors

- Two types of standing axis errors
 - Tilt in the trunnion axis
 - Mis-mounting of the laser (telescope) on the trunnion axis



PSD to Tracker Errors

- At zenith the lateral motion Δu cannot translate into a horizontal angle, but instead translates to a standing axis error.
- Δu needed to be allocated between the azimuth component, $\Delta\theta$, and a standing axis component, $\Delta\xi$.
 - $\Delta\theta \approx \frac{1}{r} \cdot \Delta u \times \sin(\varphi)$
 - $\Delta\varphi \approx \frac{1}{r} \cdot \Delta v$
 - $\Delta\xi \approx \frac{1}{r} \cdot \Delta u \times \cos(\varphi)$
- Δu and Δv are preserved
 - $\Delta\theta^2 + \Delta\varphi^2 + \Delta\xi^2 = \frac{\Delta u^2}{r^2} + \frac{\Delta v^2}{r^2}$



D-H Transforms

- D-H Transforms are a method for creating kinematic equations
 - The following is a simple tracker model
- $Rz(\theta) \cdot Ry(\varphi) \cdot T(0,0,\rho)$

$$= \begin{vmatrix} \cos(\varphi) \cos(\theta) & -\sin(\theta) & \cos(\theta) \sin(\varphi) & \rho \cos(\theta) \sin(\varphi) \\ \cos(\varphi) \sin(\theta) & \cos(\theta) & \sin(\theta) \sin(\varphi) & \rho \sin(\theta) \sin(\varphi) \\ -\sin(\varphi) & 0 & \cos(\varphi) & \rho \cos(\varphi) \\ 0 & 0 & 0 & 1 \end{vmatrix}$$

- Note that the last column corresponds to a spherical to cartesian transform



D-H Transform

- The standing axis error is modeled by adding a tilt in X after the zenith axis and before the translation to the SMR
- $Rz(\theta) \cdot Ry(\varphi) \cdot Rx(\xi) \cdot T(0,0,\rho)$
- $X(\rho, \theta, \varphi, \xi) = \rho(\cos(\theta) \sin(\varphi) \cos(\xi) + \sin(\theta) \sin(\xi))$
- $Y(\rho, \theta, \varphi, \xi) = -\rho(\sin(\theta) \sin(\varphi) \cos(\xi) + \cos(\theta) \sin(\xi))$
- $Z(\rho, \theta, \varphi, \xi) = \rho \cos(\varphi) \cos(\xi)$

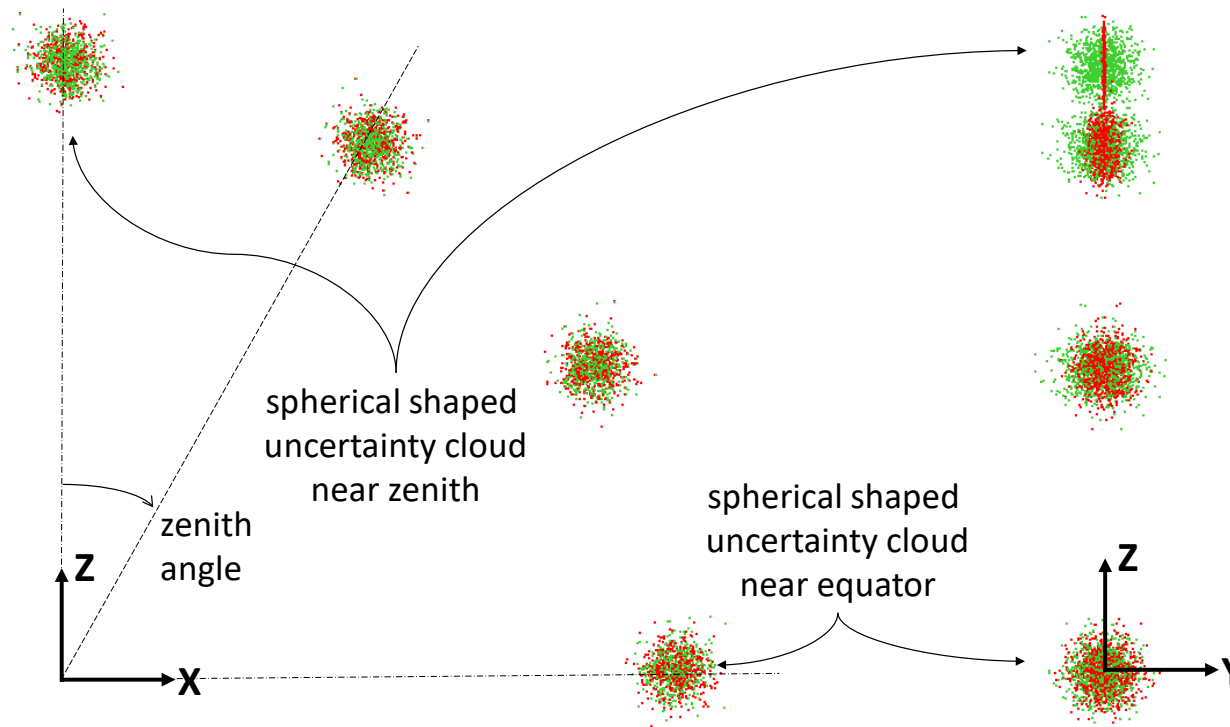


Monte Carlo

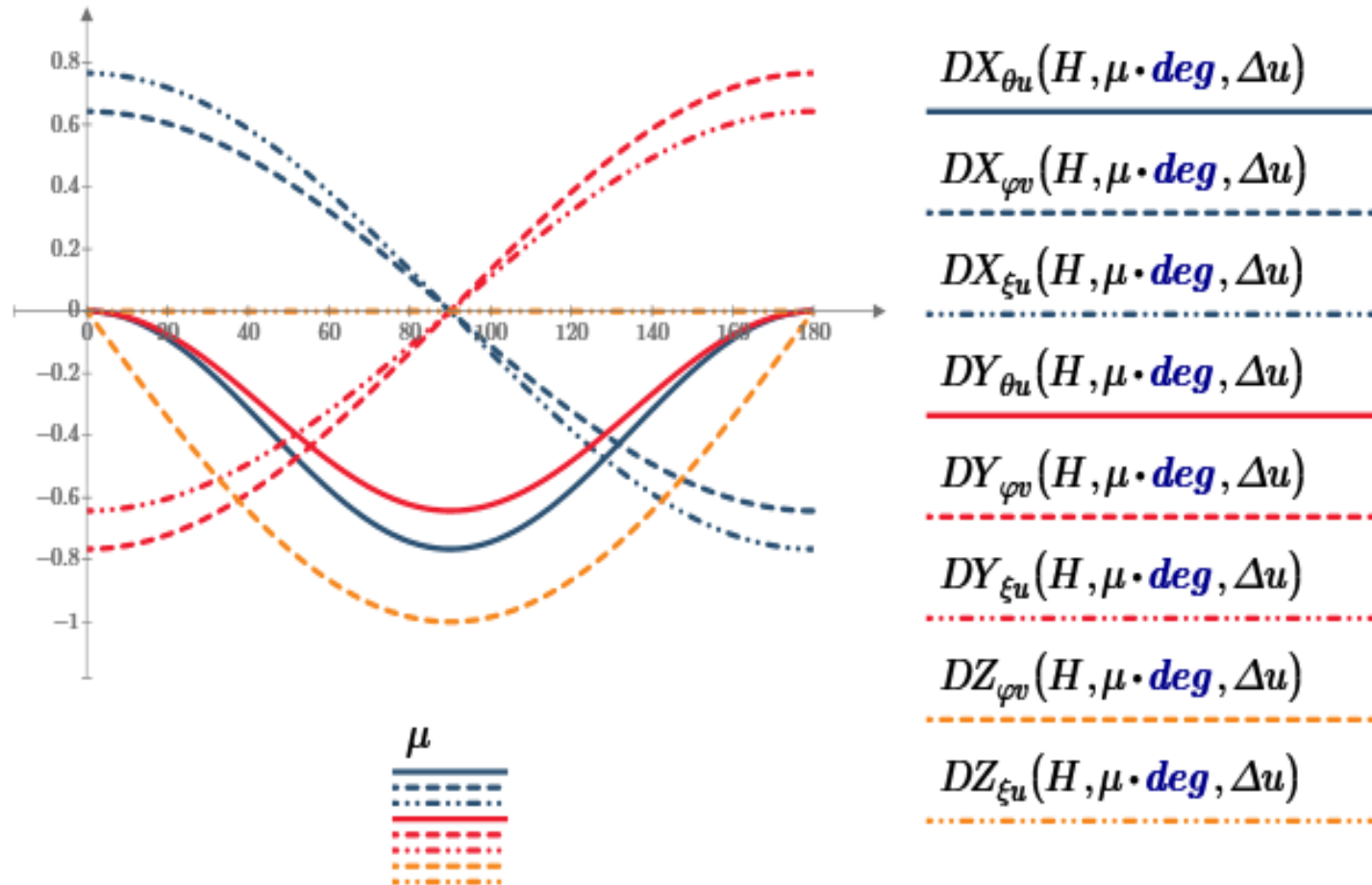
- Define the Monte Carlo errors
 - $\theta \rightarrow \theta + \Delta\theta \cdot \sin(\varphi) = \theta + \frac{\Delta u}{r} \sin(\varphi)$
 - $\varphi \rightarrow \varphi + \Delta\varphi = \varphi + \frac{\Delta v}{r}$
 - $\xi \rightarrow \Delta\theta \cos(\varphi) = \frac{\Delta u}{r} \cos(\varphi)$
 - $r \rightarrow r + \Delta r$

Monte Carlo

- Point clouds for 1000 trials

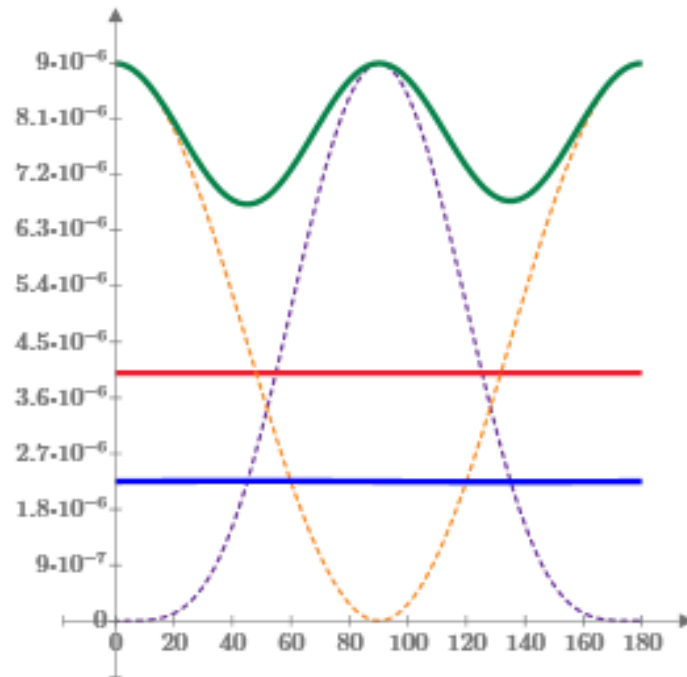


Linear Propagation of Errors



Linear Propagation of Errors

- Squaring and grouping derivative terms, and multiplying by the square of the uncertainties



$$D2_{\theta}(H, \mu \cdot \mathbf{deg}, \Delta u) \cdot \Delta u^2$$

$$D2_{\varphi}(H, \mu \cdot \mathbf{deg}, \Delta u) \cdot \Delta v^2$$

$$D2_{\xi}(H, \mu \cdot \mathbf{deg}, \Delta u) \cdot \Delta u^2$$

$$D\theta\xi^2(H, \mu \cdot \mathbf{deg}, \Delta u) \cdot \Delta u^2$$

$$D2_{\rho}(H, \mu \cdot \mathbf{deg}, \Delta u) \cdot \Delta \rho^2$$

μ



Point-to-Point Comparison

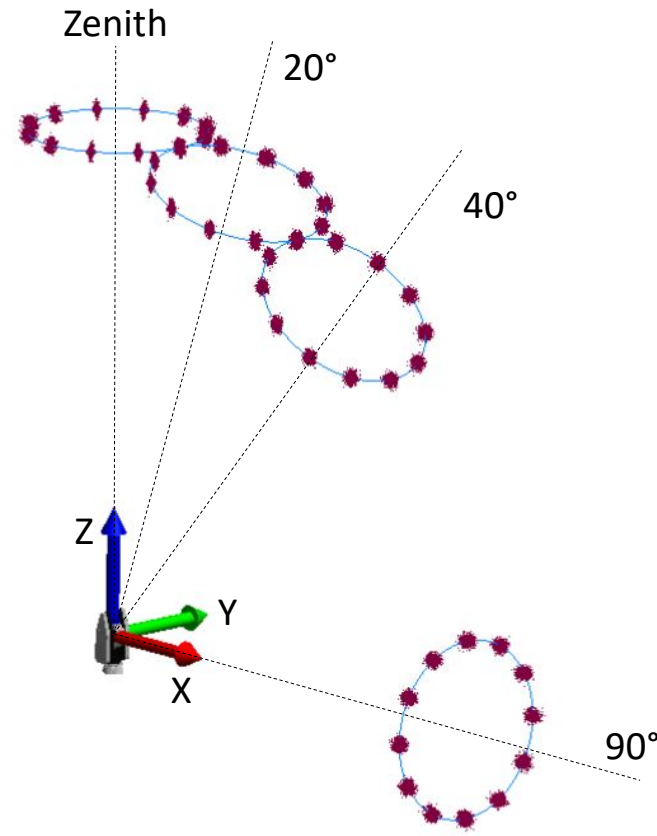
New Model:
U = 0.01
Range = 0.05

Disk Model:
U = 0.00
Range = 0.01

New and Disk Models:
U = 0.01
Range = 0.05



Points-to-Objects Comparison



Points-to-Object Comparison

- Solutions for Spherical to Cartesian and New Models are the same
- Standard Deviations are different
 - New model has larger Standard Deviation in some cases
- The analysis of disk and spherical shaped uncertainty clouds using points-to-circles evaluation in above figure is specific to that figure.

	<i>unconstrained Radius</i>			
	<i>disk point cloud</i>		<i>spherical point cloud</i>	
	<i>value (mm)</i>	<i>Stdev (mm)</i>	<i>value (mm)</i>	<i>Stdev (mm)</i>
	<i>zenith</i>		<i>zenith</i>	
X	0.0000	0.0055	0.0000	0.0055
Y	0.0000	0.0056	0.0000	0.0056
Z	3939.2310	0.0111	3939.2310	0.0111
Radius	694.5930	0.0038	694.5930	0.0038
	<i>20 deg</i>		<i>20 deg</i>	
X	1347.2964	0.0061	1347.2964	0.0066
Y	0.0000	0.0041	0.0001	0.0056
Z	3701.6663	0.0109	3701.6663	0.0109
Radius	694.5930	0.0033	694.5929	0.0041
	<i>40 deg</i>		<i>40 deg</i>	
X	2532.0890	0.0080	2532.0890	0.0082
Y	0.0000	0.0045	0.0000	0.0053
Z	3017.6260	0.0092	3017.6260	0.0093
Radius	694.5930	0.0034	694.5930	0.0040
	<i>90 deg</i>		<i>90 deg</i>	
X	3939.2310	0.0111	3939.2310	0.0111
Y	0.0000	0.0056	0.0000	0.0055
Z	0.0000	0.0056	0.0000	0.0056
Radius	694.5930	0.0039	694.5930	0.0040

Conclusion

- New model for point cloud uncertainty for spherical measurement was shown
 - On-LOS and off-LOS rays were treated differently
 - Monte Carlo uncertainty clouds stayed constant at all horizontal and zenith angles
 - Linear error propagation also stays constant at all angles
- On-LOS measurement values match other models
- Off-LOS uncertainties can differ from other models
 - Uncertainties are task specific
 - Compared to Monte Carlo methods the new model may converge more slowly than spherical to cartesian model

Acknowledgements

- Thanks also to Scott Sandwith, New River Kinematics, for discussion and suggestions for improving the paper.
- Thanks to the Large Synoptic Survey Telescope for putting me back on track and looking at this uncertainty issue again.

References

- Hammersley, J.M., Handscomb, D.C., “Monte Carlo Methods”, Methuen & Co. Ltd, London, 1964.
- “Evaluation of measurement data — Supplement 2 to the “Guide to the expression of uncertainty in measurement” — Extension to any number of output quantities”, JCGM 102:2011
- Dorsey-Palmateer, J.W., “Spinning Mirror Laser Radar Kinematic Errors”, Large Volume Metrology Conference, 2012.
- Hayden, J., Khreishi, M., Hadjimichael, T., and R. Ohl, R., “Monte Carlo Method for Uncertainty Propagation in JWST Metrology Databases”, Coordinate Metrology Society Conference, 2014.
- Calkins, J., Sandwith, S., “Integrating Certified Lengths to Strengthen Metrology Network Uncertainty”, Coordinate Metrology Society Conference, 2007.
- Brown, E.B., “Modern Optics”, Reinhold Publishing Corp, 1965.
- McGillem, C.D., Cooper, G.R., "Continuous and Discrete Signal and System Analysis", Holt, Rinehard, and Winston, Inc., 1974.
- Kam C. Lau, Robert J. Hocken, "Three and five axis laser tracking systems ", US Patent 4714339, December 22, 1987.
- Lawrence B. Brown, David N. Wells, J. Bradford Merry, "Tracking laser interferometer", US Patent 4790651, December 13, 1988.
- Paul, R.P., "Robot Manipulators", MIT Press, 1981.
- Shui, R., Kang, S., Han, J.H., Hsieh, M., "Modeling Systematic Errors for the Angle Measurement in a Virtual Surveying Instrument", J. Surveying Eng., Aug 2011.
- Palmateer, J.W., “Those #%&!\$ Corner Cubes”, Coordinate Metrology Society Conference, 2002.
- Kreyszig, E., “Advanced Engineering Mathematics 10th Edition”, J. Wiley and Sons, 2011.